Energy & Buildings 347 (2025) 116403

Contents lists available at ScienceDirect

Energy & Buildings

journal homepage: www.elsevier.com/locate/enb

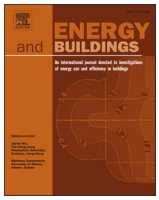

Day-ahead TCLs dispatch optimization: An integer genetic algorithm approach based on microgrids composition☆

Jesus Clavijo-Camacho *, Gabriel Gomez-Ruiz, J.A. Hernández Torres, Reyes Sanchez-Herrera

Department of Electrical Engineering of University of Huelva - Huelva, Spain

ARTICLE INFO

Keywords:
Day-ahead microgrid optimization
Genetic algorithms
Optimal scheduling
Demand response approach

ABSTRACT

Day-ahead microgrid optimization has been extensively studied in recent technical literature, which predominantly focuses on microgrids comprised of loads, renewable energy systems (RES), and energy storage systems (ESS). However, many microgrids are only composed of loads (such as homes in buildings). This work studies microgrid optimization through a specific focus on thermostatically controllable loads (TCLs), prevalent components in such microgrids. The optimization objectives are tailored to account for the unique characteristics of each microgrid's composition. Additionally, the study considers the TCLs' ability to participate in demand response programs within the power system and addresses challenges stemming from discrepancies between day-ahead dispatch and real-time operation. Importantly, the optimization process employs a genetic algorithm (GA) to derive optimal on/off sequences and corresponding temperature profiles for each TCL, instead of adjusting variable temperature setpoints. Furthermore, the GA initial population is generated using a novel method called stratified random sampling, proposed in this work. The study presents a procedure for TCL optimization aimed at maximizing each microgrid's performance relative to its composition. Results demonstrate a reduction in the targeted metric ranging from 2.4% to 18%.

1. Introduction

In recent years, there has been a notable shift in the global energy landscape towards increasing reliance on renewable energy sources, driven by efforts to address the challenges posed by traditional power generation methods [1]. The rise of renewables is evident in significant milestones, such as Europe's substantial increase in renewable energy generation, accounting for nearly 41 % of total power generation in 2022 [2]. According to projections from the International Energy Agency, solar photovoltaic (PV) and wind power are expected to contribute substantially to global power generation by 2030, accounting for about 40 % of building electricity usage [3]. However, the integration of intermittent renewable energy sources, such as solar and wind, into the power system presents new challenges. The rapid variability of renewable energy generation can lead to mismatches between supply and demand, resulting in potential disruptions to the grid, including voltage fluctuations and power outages [4]. These challenges underscore the importance of implementing strategies to enhance grid resilience and ensure reliable electricity supply.

One promising approach to address these issues are the demand response programs [5], which involve intelligently managing electricity consumption to align with supply dynamics or grid requirements [6]. Within the framework of demand response, Thermostatically Controlled Loads (TCLs) emerge as a valuable tool due to their inherent flexibility in adjusting energy consumption patterns [7 8]. The deployment of TCLs not only aids in balancing grid demand and supply but also presents an opportunity to optimize overall installation performance, particularly within microgrids framework. By implementing tailored optimization objectives based on the specific composition of the microgrid, TCLs can not only respond to grid dynamics but also contribute to enhancing the overall efficiency [9] and stability of the microgrid.

This study aims to underscore the significance of TCLs in optimizing energy consumption and reducing costs within a microgrid, while ensuring their availability for system supervision and responsiveness to demand-side management.

☆ This article is part of a special issue entitled: 'Decarbonising Built Env' published in Energy & Buildings.

* Corresponding author.
E-mail address: jesus.clavijo@die.uhu.es (J. Clavijo-Camacho).

https://doi.org/10.1016/j.enbuild.2025.116403
Received 29 July 2024; Received in revised form 12 July 2025; Accepted 3 September 2025
Available online 5 September 2025

Table 1
Comparison table of related works.

Ref.	TCL used				Microgrid contain		Optimization algorithm	Control variable	DR consideration
	AC	Fridge	Freezer	EWH	ESS	RES			
This work	✔	✔	✔	✔	✔	✔	GA	ON/OFF sequence	✔
[7]	✔	✘	✘	✘	✔	✔	MILP[a]	cooling capacity, Qc	✔
[9]	✔	✘	✘	✘	✔	✔	PSO[2]	load shifting & curtailment logic	✔
[10]	✔	✔	✔	✔	✘	✘	MILP[a]	VESS model ON/OFF	✔
[11]	✔	✘	✘	✘	✘	✘	Rule-based control (price-responsive thermostat)	Temperature setpoint	✔
[12]	✔	✘	✘	✔	✔	✔	Linear Programming	Heating power	✔
[13]	✘	✔	✔	✘	✔	✔	MIQP[3] + Decentralized Gradient Descent	ON/OFF sequence	✔
[18]	✔	✘	✘	✔	✘	✘	NSGA[4] III	Temperature setpoint	✘
[24]	✔	✘	✘	✔	✔	✔	MILP[a]	Heating power	✔
[50]	✘	✘	✘	✔	✘	✘	Linear Programming	Temperature setpoint	✘
[51]	✔	✘	✘	✘	✔	✔	Approx. Dynamic Programming	Temperature setpoint	✘
[52]	✔	✘	✘	✔	✔	✔	Quadratic Programming	Temperature setpoint	✔
[53]	✔	✘	✘	✘	✘	✘	MILP[a]	ON/OFF sequence	✔

[a] Mixed-Integer Linear Programming, [2] Particle Swarm Optimization, [3] Mixed-Integer Quadratic Programming, [4] Non-dominated Sorting Genetic Algorithm.

1.1. State of art

Papers published in the technical literature can be divided in two approaches: those which present methods to optimize the consumption/expense of TCLs and those other which study the possible use of TCLs to balance offer and demand in the power system. Table 1 shows a comparison between the different studies similar to this presented work.

Prior to the use of TCLs in any of the approaches indicated above, their model is an important step addressed by many studies in the technical literature. These models typically involve differential equations that capture heat transfer dynamics between the appliance, the enclosed space it regulates, and the surrounding environment. Among the most common TCLs, which constitute approximately 90 % of those found in typical installations, are the fridge, the freezer, the electric water heater (EWH), and the air conditioner. In Section 2, models are presented for each of these TCLs, explaining the rationale behind their selection and highlighting their adaptability to different scenarios.

On the one hand, within the approach of optimizing the consumption/expense of the TCLs, they can serve as versatile tools for energy optimization within microgrids due to their inherent flexibility, allowing them to be adjusted [10]. The strategies, established in advance (day-ahead), enable these systems to follow pre-defined dynamics, thereby achieving efficient energy utilization. Day-ahead scheduling is widely used for optimal TCL dispatch, considering energy prices [11], user comfort [12] and appliance power profile [13 14]. Several studies have addressed the problem formulation using various algorithms, as discussed in Section 4.4. To address uncertainties stemming from RES, electricity prices, and human behaviour factors, researchers are exploring stochastic programming methods, which offer robust solutions to optimize TCL operation in dynamic and uncertain environments. [15 16 17 18]. Emerging optimization techniques, including machine learning algorithms [19] or hybrid Fuzzy/Markov Chain-based [20 21], hold promise for further enhancing TCL optimization strategies. During operation, disturbances in the systems are best corrected to maintain optimization using tools such as Predictive Control techniques [22]. Particularly, Model Predictive Control (MPC) [23 24] enables proactive optimization by utilizing TCL dynamic models to predict future behaviour under various control settings. Most previously published provide an optimization based on the temperature.

On the other hand, the use of TCLs in demand response (DR) programs could play a pivotal role in the dynamic management of electricity consumption, allowing grid operators to actively engage with consumers to adjust their electricity usage in response to grid conditions and market signals [25 26]. TCLs are well-suited to participate in demand response programs due to their inherent characteristics:

- **Versatility/flexibility** in adjusting their energy consumption patterns without compromising user comfort [27].
- **Large-Scale Deployment,** enabling substantial aggregate capacity via aggregators and hierarchical coordinated control methods [28]: centralized [29] and decentralized [30 31].
- **Predictable Behaviour** based on predefined models as previous commented [32].
- **Cost-Effectiveness,** enabling grid operators to reduce peak demand without significant infrastructure investments [33], automatically and remotely control [34] while also providing users with rewards [35].

One of the most common approaches to manage TCLs in DR scenarios is through their modelling [36], often likened to virtual energy storage systems known as Virtual Energy Storage Systems (VESS) [37 38]. Within this framework, TCLs are effectively represented as energy storage units, where charging and discharging actions are manifested by adjusting the setpoint temperature of the targeted TCL. This temperature modulation corresponds to the processes of increasing or decreasing energy consumption, thereby facilitating controlled energy release or absorption in alignment with grid demand dynamics. Although this approach removes users' direct control over their own TCLs, the energy handling capabilities of TCLs have been extensively investigated in the literature, as well as their equivalence in aggregation [37]: direct aggregation methods [39], temperature priority list algorithm [40] and state space method [41].

From the state of art carried out, it can be concluded these research gaps:

- The lack of integrated methods that simultaneously address both optimization and demand response requirements.
- The existing research primarily focuses on optimizing microgrid Energy Management Systems (EMS), overlooking the dedicated optimization of TCLs as standalone entities within those microgrids that invariably incorporate them.
- The absence of adaptive objective functions in optimization formulations tailored to the specific microgrid context of TCLs, failing to differentiate between microgrid compositions, including microgrids solely composed of TCLs.
- The limited consideration of the collective operation of multiple TCLs (such as fridge, freezer, AC, and EWH) within the optimization framework.
- The no scalability of TCL models used in optimization to different scenarios, characterized by the opaque nature of parameters hindering their adaptability to diverse users' installations.

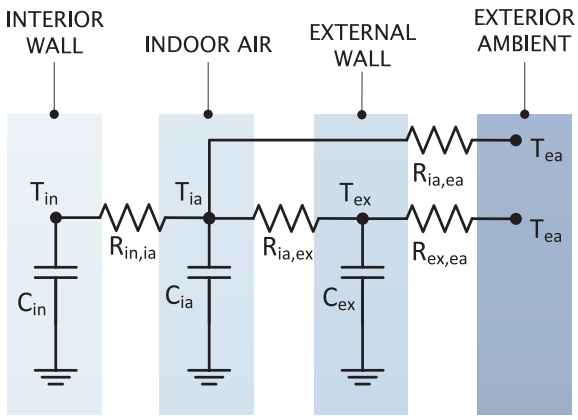

Fig. 1. Thermal network chosen for the electric space heating/cooling.

Table 2
Electric space heating/cooling parameters.

Parameter	Unit	Value
$R_{in,ia}$	KW^{-1}	7×10^{-3}
$R_{ia,ex}$	KW^{-1}	7×10^{-3}
$R_{ex,ea}$	KW^{-1}	1×10^{-1}
$R_{ia,ea}$	KW^{-1}	1×10^{-2}
C_{in}	JK^{-1}	5×10^{2}
C_{ex}	JK^{-1}	2×10^{2}
C_{ia}	JK^{-1}	8×10^{1}

1.2. Work contributions

Compared with previous studies, the main contributions of this work are summarized below:

- A day-ahead optimization strategy based on a novel ON/OFF profile generation approach, leveraging an integer GA.
- Tailored objective functions formulated to address the specific composition of the microgrid (TCLs and/or RES/ESS), as presented in Section 3. This optimization approach considers the collective operation of multiple validated and state-of-the-art TCL models (such as fridge, freezer, AC, and EWH).
- A novel initial population creation strategy in the GA, employing stratified sampling, is proposed, providing improved results (detailed in Section 4).
- Implementation of the proposed double-band temperature concept, which includes the operating temperature hysteresis band (THB) and the comfort THB, to keep the microgrid available for participation in DR programs (detailed in Section 5).
- This ON/OFF approach facilitates the design of a supervisor (explained in Section 6), capable of addressing mismatches arising from unforeseen events.

1.3. Paper organization

The paper is organized as follows: Section 2 discusses the theoretical foundations of thermostatically controlled load models considered in the optimization framework and their significance. Section 3 outlines the problem framework. Section 4 presents the optimization problem along with its constraints, objective functions, etc. Sections 5 and 6 address the consideration of demand-response strategy and real-time mismatches, respectively. In Section 7, a scenario is proposed for optimization, covering various compositions that may exist within the microgrid, comparing them with the unoptimized baseline case. Finally, Section 8 outlines the conclusions drawn from the study.

2. Thermostatically controlled load models

Our research adopts an approach to selecting models for TCLs which emphasize their suitability for optimization problems. Rather than employing complex models prevalent in the literature [42,43,44], models of reduced order and fewer parameters are prioritized, striking a balance between accuracy and interpretability. This choice not only simplifies implementation but also minimizes the computational resources required for model execution. Moreover, by following a grey-box approach, where parameters are approximated based on physical principles and refined through experimental data, the models offer enhanced interpretability compared to a black-box model approach [45,46]. In this way, the gap between theoretical understanding and empirical validation is bridged, resulting in parameter estimation closely aligned with real-world values. For example, to show that accuracy is important to choose the different models, note that the order of fridge and freezer models are different even though the composition of both TCLs is quite similar, and a high order model has been used to represent the freezer, [47,48].

A hybrid modelling approach that combines two complementary models is presented. On the one hand, the operation of the TCL is represented as a binary on/off model, which simplifies the modelling process. On the other hand, a more detailed representation of TCL behaviour is achieved by employing a model that integrates thermal resistances (R) to represent impediments to heat transfer (e.g., the thermal insulation between the room and the building wall), and thermal capacities (C) to denote the ability to retain energy in form of heat in a thermal node (e.g., the room's capacity to absorb heat). Therefore, each TCL considered in this study is modelled following the grey-box hybrid approach based on RC circuits. The models are formulated using the discrete time state-space representation.

$$\dot{\boldsymbol{x}}(k) = \boldsymbol{A}(\theta)\boldsymbol{x}(k) + \boldsymbol{B}(\theta)\boldsymbol{u}(k) \tag{1}$$

$$\boldsymbol{y}(k) = \boldsymbol{C}\boldsymbol{x}(k) \tag{2}$$

Equation (1) outlines the thermodynamic analysis of the TCL, resulting in a system with many first-order differential equations, corresponding to the number of energy storage elements in the model, i.e., thermal capacities. As for the Equation (2), it represents the output equations of the state-space model and can be observed that it is not dynamic and is determined by the designer, typically using an output vector $\boldsymbol{y}(k)$, which contains coordinates corresponding to the measurable variables of interest.

In detail, k represents the sampling, $\boldsymbol{x} \in \mathbb{R}^n$ is the state vector, where n is the order of the model (the number of first-order differential equations) and is constituted by the temperature of the nodes considered in the model, $\boldsymbol{u} \in \mathbb{R}^p$ is the input vector, where p is the number of inputs, and includes external parameters that affect the TCL behaviour as the ambient temperature Tamb, the power consumed by the TCL, the solar irradiance Is in the case of the air conditioner, or the water ambient temperature Tw in the case of the EWH. $\boldsymbol{A} \in \mathbb{R}^{n \times n}$ is the state matrix, $\boldsymbol{B} \in \mathbb{R}^{n \times p}$ is the input matrix, and $\theta \in \mathbb{R}^m$ is the vector of m model parameters. Regarding the Equation (2), $\boldsymbol{y} \in \mathbb{R}^q$ is the output vector, where q is the number of outputs, and $\boldsymbol{C} \in \mathbb{R}^{q \times n}$ is the output matrix.

Subsequently, utilizing the established physical principles, state-space models for each TCL included in the proposed study will be developed, as described below.

2.1. Air conditioner

This model is developed based on [49]. Three nodes are considered with each corresponding temperature, as shown in Fig. 1. The value of the different parameters is the shown in Table 2, according to [49].

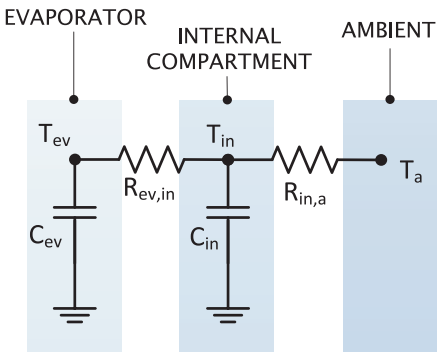

Fig. 2. Thermal network chosen for the fridge.

Table 3
Frigde parameters.

Parameter	Unit	Value
$R_{ev,in}$	KW^{-1}	9.0348×10^{-1}
$R_{in,a}$	KW^{-1}	9.0188×10^{-1}
C_{ev}	JK^{-1}	3.4342×10^{2}
C_{in}	JK^{-1}	1.1600×10^{4}

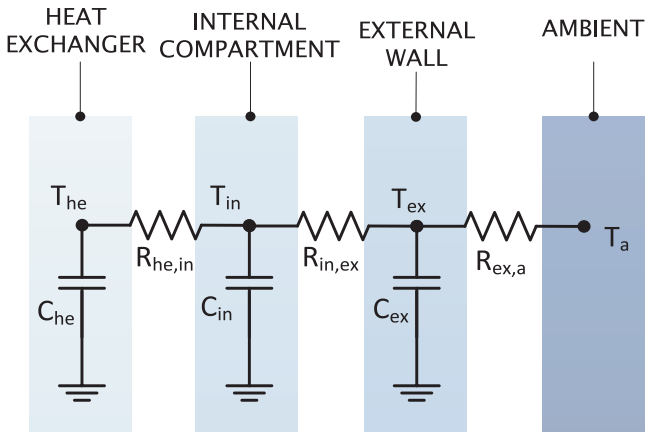

Fig. 3. Thermal network chosen for the freezer.

Table 4
Freezer parameters.

Parameter	Unit	Value
$R_{he,in}$	KW^{-1}	1.12×10^{-1}
$R_{in,ex}$	KW^{-1}	4.97×10^{-1}
$R_{ex,a}$	KW^{-1}	1.28×10^{-1}
C_{he}	JK^{-1}	1.05×10^{3}
C_{in}	JK^{-1}	4.76×10^{3}
C_{ex}	JK^{-1}	8.11×10^{3}

Table 5
Electric water heater parameters.

Parameter	Unit	Value
R_w	KW^{-1}	1.52×10^{-3}
C_w	JK^{-1}	863.4×10^{3}

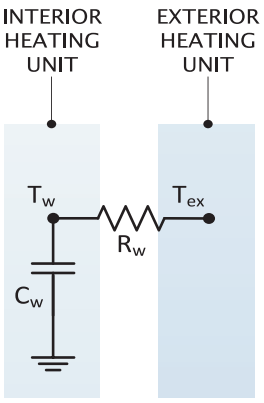

Fig. 4. Thermal network chosen for the electric water heater when there is no hot water consumption.

2.2. Fridge

The development of this model is based on [47]. In [47] several models for a fridge are presented and compared. The authors conclude that the best results are the provided by the linear- second order model, which is the chosen in the present work. The equivalent RC circuit is shown in Fig. 2, with the corresponding parameter values listed in Table 3.

2.3. Freezer

In this case, the model has been chosen based on [48]. As in the case of the fridge, in [48] a comparison between several freezer models are presented and the linear three order model is chosen as the best. That is the elected in the present work as shown in Fig. 3. The values of the different parameters are presented in Table 4.

2.4. Electric water heater (EWH)

In this system, two scenarios are considered: one without hot water consumption and one with hot water consumption. As a result, two different models are developed based on [18] and [50]. In the first scenario, when there is not hot water consumption, two external variables are considered: the exterior temperature of the water heater housing and the electrical power used for heating. In the second scenario, when there is hot water consumption, only one external parameter is considered: the volume of hot water consumed. Model parameters values are listed in Table 5. The RC model for the electric water heater, when there is not hot water consumption, is shown in Fig. 4.

3. Problem Overview

The objective of this study is to optimize TCL operation while ensuring certain power reserve to participate in the demand response process at any time. The optimization is established through a comprehensive ON/OFF sequence for the following day. To achieve this, a total of 1440 operational instructions (24 h x 60 min) will be assigned for each TCL. This is made possible through the utilization of system models encompassing AC-rooms, Fridge-room, Freezer-room, and EWH-room, and their response to changes in temperature and the other external variables, by adapting every TCL model parameter presented in section 2. As can be observed in the models, these systems are influenced by parameters that can be reliably estimated for the following day, such as ambient temperature and irradiance. Another crucial factor affecting the optimization process is the electricity tariff for the subsequent day, a parameter that is typically known in advance in the European context. This pricing information plays a pivotal role in determining the optimal operation strategy for the TCLs, as it directly influences their scheduling

Table 6
μgrid composition influence into optimization objectives.

Microgrid composition	Objective pursued	Description
TCL	Obj. 1	Minimizing TCLs energy cost
TCL + ESS	Obj. 2	Reducing TCLs power consumption
TCL + RES	Obj. 3	Optimizing a trade-off between cost and power consumption based on the production of RES.
TCL + ESS + RES	Obj. 4 ≡ Obj. 2	Reducing TCLs power consumption

decisions and overall energy consumption pattern.

For effective optimization, understanding the composition nature of the microgrid is imperative, as it can influence the optimization mode of the TCL, or equivalently, the objective pursued by this problem.

Hence, if TCL is the sole entity used to optimize the microgrid performance, it becomes essential to customize the objective function of the problem based on the microgrid's composition. Four combinations must be considered: microgrids consisting solely of TCLs, those with TCLs and ESS, those with TCLs and RES, and those with TCLs, RES, and ESS. Table 6 summarizes the issue.

4. Optimization problem formulation

The optimization problem is formulated as follows:

4.1. Decision variable

The decision variables for this optimization problem consist of the ON/OFF states of the different TCLs considered in the microgrid. This approach is preferred over altering the hysteresis bands repeatedly, as it offers a more stable and predictable control strategy. Unlike adjusting hysteresis bands, which can lead to frequent fluctuations in operation, maintaining predetermined ON/OFF sequences ensures consistent and efficient operation of the TCLs. In addition, the chosen procedure facilitates the correction of mismatches caused by forecast errors. Therefore, the value of this variable can only be 0 or 1.

$$DecisionVariables\begin{cases} U_{fridge}(t) \\ U_{freezer}(t) \\ U_{AC}(t) \\ U_{ewh}(t) \end{cases} \tag{3}$$

4.2. Objectives

The objectives of the optimization problem are formulated based on the specific composition of the microgrid, as detailed in Section 3. These objectives encompass minimizing TCL energy costs, reducing TCL power consumption, or optimizing a trade-off between cost and power consumption based on the production of RES, such as photovoltaics, which are directly influenced by irradiance levels. By leveraging this relationship, the optimization process can effectively consider the operational costs during periods of abundant RES production, thereby enhancing energy efficiency and cost-effectiveness. Each objective is quantified as following.

Obj. 1 – minimizing TCLs energy cost

The objective function for minimizing TCLs energy costs is formulated as:

$$\text{Minimize } C = \sum_{n=1}^{N} P_{TCL} \bullet U_{TCL}(t) \bullet price(t) \bullet \Delta t \tag{4}$$

Where C is the total energy cost over the optimization horizon from $n = 1$ to N. N represents the total number of time intervals in the optimization horizon. This value is calculated by multiplying 24 h by 60 min, resulting in 1440 intervals. Δt represents the time step (discretization between each interval) and remains 60 s, indicating the duration of each time interval as it considers a minute-by-minute approach. P_{TCL} is the power consumption of the TCL that $U_{TCL}(t)$ ON/OFF sequence over the time is going to be optimize. $Price(t)$ is the electricity price at time t.

Obj. 2 – reducing TCLs power consumption

The objective function for reducing TCLs power consumption over the optimization is formulated similarly to the energy cost minimization objective, but without considering the electricity price component.

$$\text{Minimize } C = \sum_{n=1}^{N} P_{TCL} \bullet U_{TCL}(t) \bullet \Delta t \tag{5}$$

Obj. 3 – optimizing a trade-off between cost and power consumption based on the production of RES

The objective function for optimizing the trade-off between cost and power consumption based on RES production, is formulated as:

$$\text{Minimize } C = \sum_{n=1}^{N} P_{TCL} \bullet U_{TCL}(t) \bullet price(t) \bullet f(P_{RES}(t), P_{totalTCL}) \bullet \Delta t \tag{6}$$

Where:

$$f(P_{RES}(t), P_{totalTCL}) = \frac{P_{totalTCL} - P_{RES}(t)}{P_{totalTCL}} \tag{7}$$

This function quantifies the proportion of energy that can be self-supplied by the RES and can be proportionally discounted from the grid price for the optimization consideration, where $P_{totalTCL}$ denotes the total TCLs, power installed in the microgrid. $P_{RES}(t)$ is:

$$P_{RES}(t) = Is(t) \bullet A \bullet \eta \tag{8}$$

The power generated by the PV RES considered $P_{RES}(t)$ at time t is proportional to the irradiance $Is(t)$, the area of PV panels A and its performance η.

The function $f(P_{RES}(t), P_{totalTCL})$ from eq (7) serves as a cost adjustment factor within the optimization problem. It reflects the degree to which energy consumption costs can be offset by self-generated RES. At its core, this function determines the portion of TCL energy consumption costs that can be discounted based on the availability of RES. When RES generation is sufficient to cover the entirety or a portion of TCL power demand, $f(P_{RES}(t), P_{totalTCL})$ will appropriately reduce the effective energy cost associated with TCL operation during that time of period.

In mathematical terms, the optimization function adjusts the total energy cost C by multiplying it with $f(P_{RES}(t), P_{totalTCL})$ at each time step t along with the electricity price for that specific time of period. This adjustment ensures that the optimization process prioritizes the utilization of self-generated power from RES, thus minimizing reliance on external grid energy and enhancing cost-effectiveness.

By integrating this cost adjustment mechanism into the optimization framework, the algorithm can dynamically optimize TCL operation strategies to leverage available renewable energy resources effectively, ultimately contributing to improved energy efficiency and economic savings within the microgrid system.

4.3. Constraints

The next constrains must be imposed:

- The decision variable (states of TCLs) is constrained to take on only binary integer values, eq (9).

$$U_{TCL}(t) \in \{0, 1\} \tag{9}$$

- The system's temperatures from TCLs, as described in Section 2, plays a critical role influenced significantly by the decision variable, which substantially impacts the system's thermal behaviour. It dictates the calculation of the system temperature at each discrete time

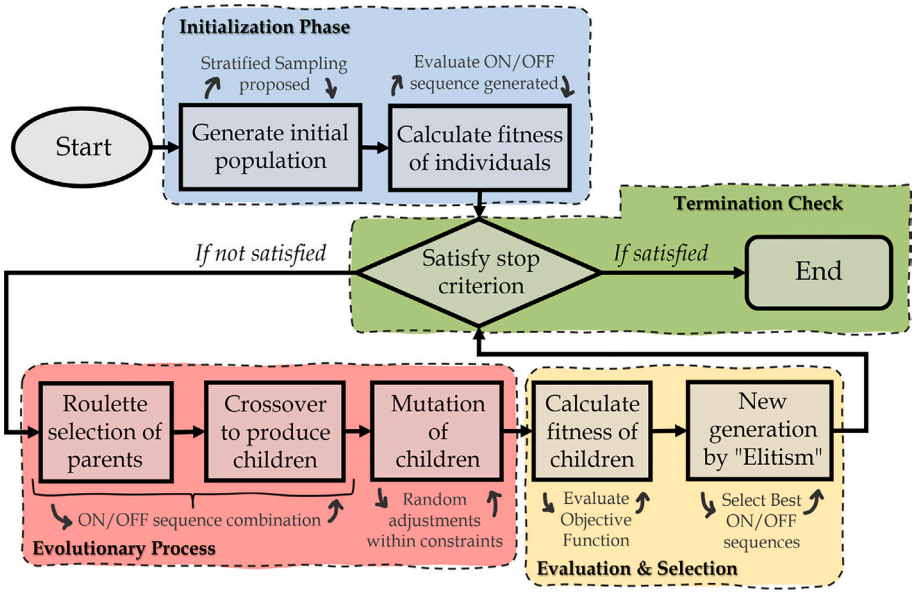

Fig. 5. Flowchart of the Genetic Algorithm applied in this study.

step t. It is imperative that at every time step t, the system temperature remains within the predefined operating temperature hysteresis band specific to each TCL.

$$T^{set}_{TCL_i} - \frac{\delta_{TCL_i}}{2} \leq T_{TCL_i}(t) \leq T^{set}_{TCL_i} + \frac{\delta_{TCL_i}}{2} \tag{10}$$

Where $T^{set}_{TCL_i}$ is the setpoint temperature for the TCL i, δ_{TCL_i} is the weight of the operating temperature hysteresis band for the TCL i and $T_{TCL_i}(t)$ is the temperature of the system modelled by the TCL i at the time step t.

4.4. Solver: Integer genetic algorithm

Since the optimization of the state of TCLs over the next 24 h, minute by minute, requires discrete integer values—specifically binary values of 1 or 0—the problem inherently assumes an integer character. While various optimization algorithms such as linear programming, local search, branch-and-bound algorithms, as well as particle swarm optimization, are commonly used, they often prove ineffective when handling integer decision variables. Therefore, algorithms designed specifically to handle integer decision variables, such as genetic algorithms (GAs), become particularly relevant. Although algorithms like the Non-dominated Sorting Genetic Algorithm (NSGA) are well-known choices for multi-objective optimizations, the problem raised entails optimizing a single objective at a time. Hence, the basic GA emerges as the preferred choice for addressing this optimization problem. However, like all metaheuristics, GAs do not guarantee finding the global minimum; instead, they converge to a local minimum. This is primarily due to the theoretical proof that reaching the global minimum is an NP-hard problem.

Additionally, it is worth noting that optimization of this type of problem can also be achieved using dynamic programming [15 51]. In fact, the authors have successfully employed dynamic programming techniques for systems of first order (i.e., involving a single state variable). However, when dealing with systems of higher order complexity, such as the freezer system (order three), dynamic programming becomes computationally prohibitive due to the substantial computational memory it demands. This is primarily attributed to the exponentially growing state space associated with higher-order systems, which escalates computational complexity. Therefore, while dynamic programming may offer an alternative approach for optimization in certain cases, its practical applicability is limited by computational constraints, particularly in systems requiring high precision and involving multiple state variables.

Considering the inherent challenges associated with the discussed optimization problems, genetic algorithms (GAs) emerge as the preferred choice for addressing such complexities.

4.4.1. Genetic algorithm workflow

A Genetic Algorithm is a population-based optimization method inspired by natural selection, commonly employed in solving combinatorial problems. Each individual in the population encodes a potential ON/OFF sequence for a TCL as a binary chromosome. The GA iteratively improves solution quality through selection, crossover, and mutation, guided by a fitness function defined as the inverse of the objective function:

$$f(x) = \frac{1}{\mathcal{F}(x) + \epsilon} \tag{11}$$

where ϵ is a small positive constant to prevent division by zero. The algorithm continues until convergence criteria are met or a maximum number of generations is reached. The overall workflow of the Genetic Algorithm and its specific adaptation to the proposed optimization problem are illustrated in Fig. 5.

Following the framework illustrated in Fig. 5, the first phase—Initialization Phase—is particularly relevant as it introduces a stratified sampling method for generating the initial population. Unlike conventional random initialization, the novel approach proposed in this work considers variations in electricity prices throughout the optimization horizon, ensuring that ON/OFF sequences are structured accordingly. This methodology is elaborated in detail in the subsequent section 4.4.1.1, where the stratified sampling process is thoroughly explained.

4.4.1.1. Initial population: Stratified randomness sampling. The establishment of the initial population is a crucial step in the Integer Genetic Algorithm (IGA) framework, as it sets the foundation for subsequent evolutionary processes. In this work, a stratified sampling approach has been adopted to generate the initial population for the IGA.

1. **Data Preparation**: The algorithm utilized the anticipated electricity prices for each hour of the following day, resulting in a total of 24 price values representing the 24-hour period.

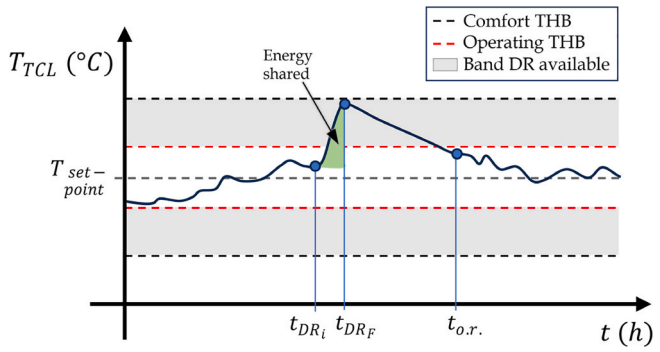

Fig. 6. Temperature Dynamics and Demand Response in TCL Systems proposed.

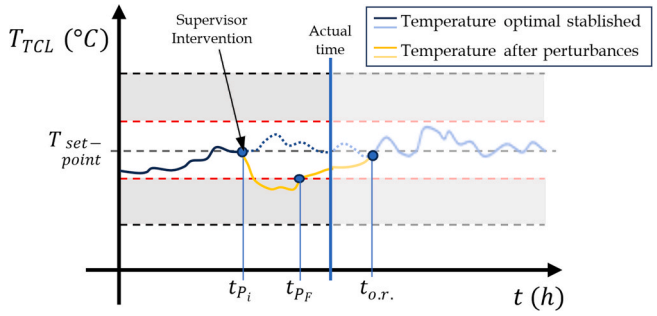

Fig. 7. Real-time operation in TCL Systems proposed.

2. **Stratification Process:** Within each population, the probability of setting the TCLs to ON or OFF at each time step was determined based on the corresponding electricity price. Specifically, when the electricity price was lower (indicating cheaper electricity), there was a higher probability of setting the TCLs to ON. Conversely, when the electricity price was higher, there was a higher probability of setting the TCLs to OFF. This stratification ensured that the initial population encompassed a diverse range of potential solutions that considered variations in electricity prices throughout the day.
3. **Population Generation**: Following the indicated in the item 2, 200 populations were randomly generated, each representing a potential input space for the optimization problem. These probabilities ensured that each population was generated considering the varying electricity prices throughout the day because, although random, they followed the stratification process. This approach guaranteed that each population contained unique configurations of ON/OFF sequences tailored to different price scenarios.

By incorporating the stratification process into the initial population generation, the optimization algorithm was equipped with a comprehensive set of starting solutions that effectively captured the influence of electricity prices on TCL operation. This approach facilitated a more robust and adaptive optimization process, enabling the algorithm to explore a diverse range of potential solutions.

4.5. *Algorithm implementation*

The proposed optimization algorithm has been implemented in MATLAB® to generate day-ahead sequential ON/OFF profiles for each TCL in the microgrid. Based on forecast data for ambient temperature, solar irradiance, water temperature, and electricity price, the algorithm optimizes TCL operation to minimize the selected objective functions

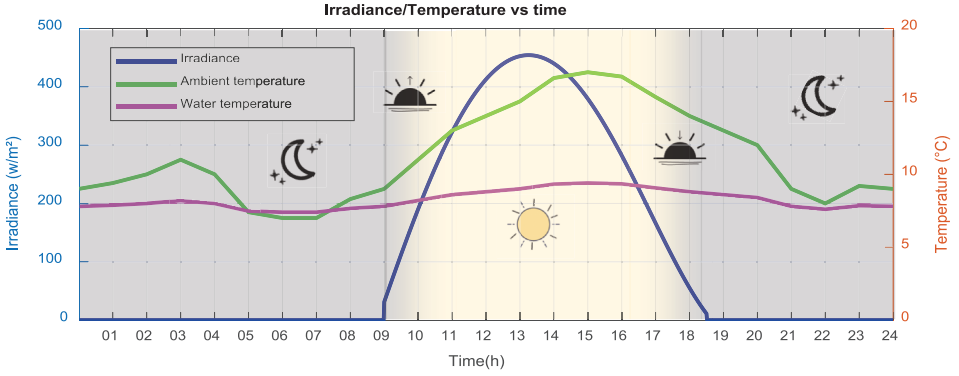

Fig. 8. External ambient conditions.

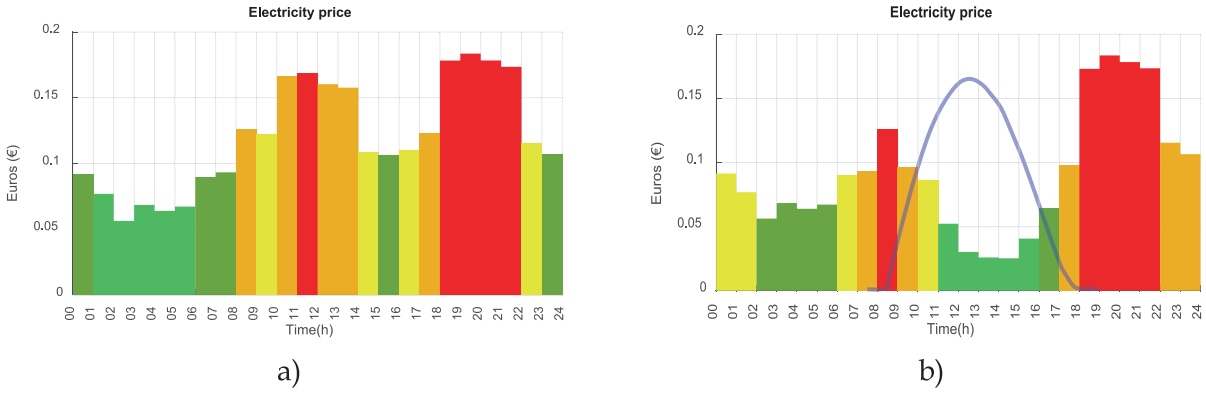

Fig. 9. Electricity price a) From the utility company b) From equivalence for optimization in TCL + RES scenario.

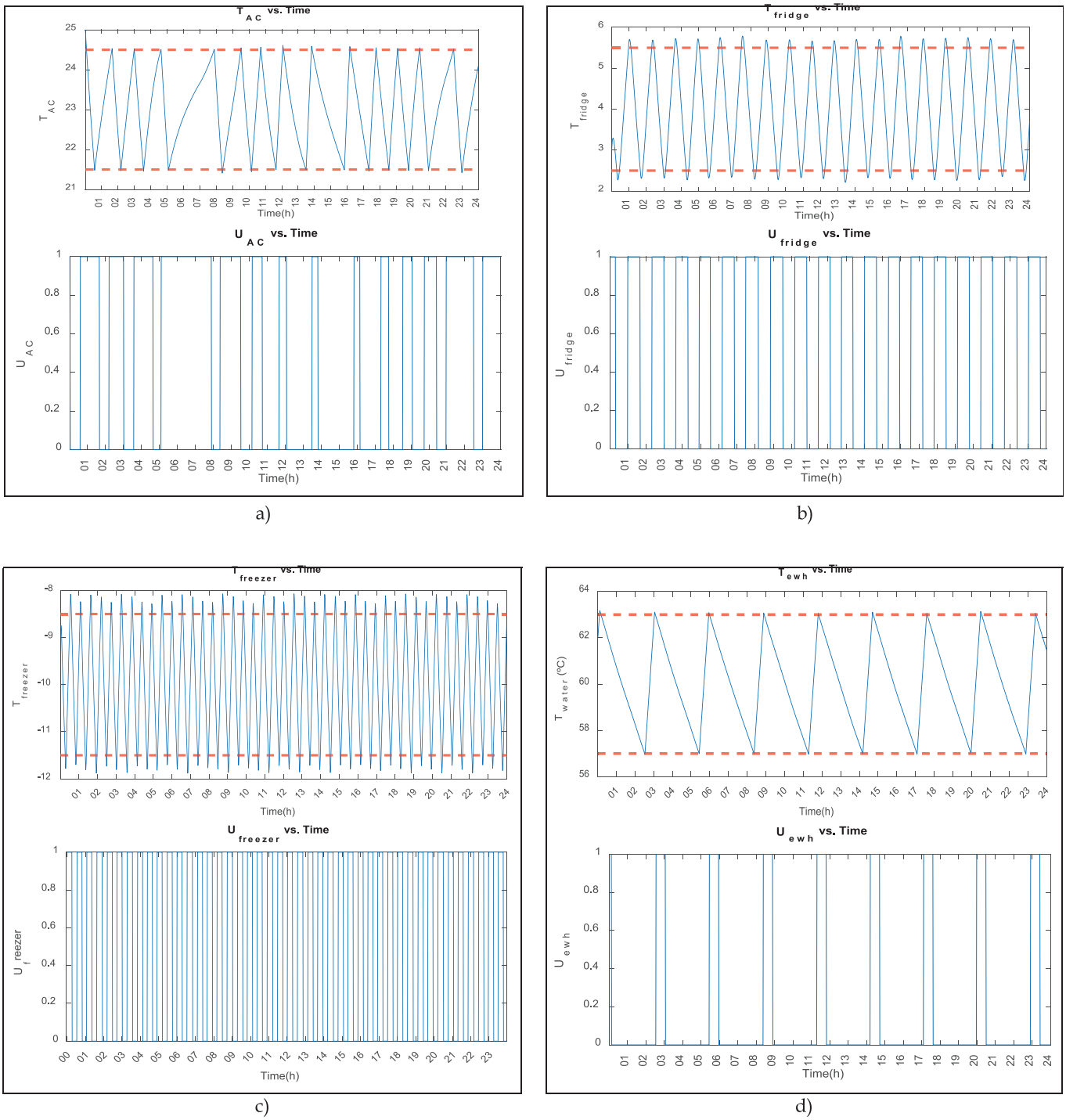

Fig. 10. Temperature dynamics and it corresponds ON/OFF sequence of a) AC b) Fridge c) Freezer d) EWH.

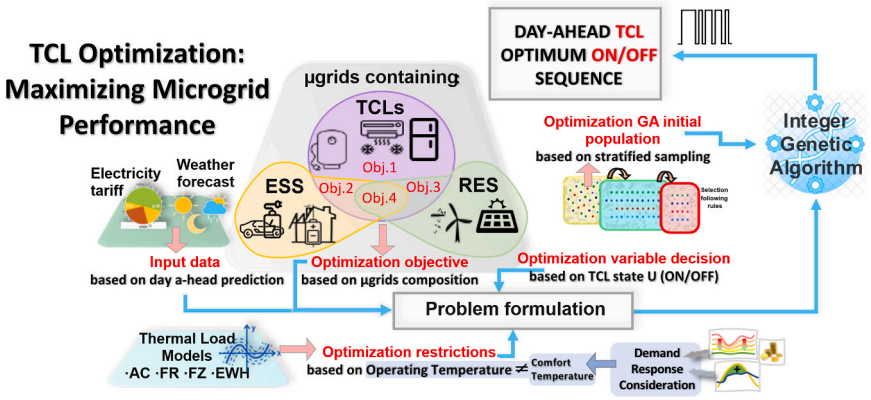

Fig. 11. Summary of the optimization process.

according to the microgrid configuration. The optimization is performed using a genetic algorithm with scenario-based constraints and binary decision variables. The process is summarized in Algorithm 1.

Algorithm 1 Pseudocode of the Optimization algorithm

BEGIN

Load forecast data (*Irradiance, Ambient Temperature, Water Temperature, Electricity Price*)
Define TCL models (*AC, fridge, freezer, EWH*) *and each parameter* [Section 2]
Define microgrid composition scenario (*TCL only, TCL + RES, TCL + ESS, TCL + RES + ESS*) [Table 6]
Define optimization problem structure (24-*hour horizon*, 1-*minute resolution*, 1440 *states*):
– *Decision variables*: *ON/OFF states* ***[Eq.(3)]***
– *Choose objective functions depending on μgrid composition* ***[Eq.(4), Eq.(5), or Eq.(6)& (7)]***
– *Constraints on thermal behaviour and binary variables* ***[Eq.(9)&(10)]***
– *Initial population generated via stratified sampling based on electricity prices*
FOR *each TCL* (*starting with AC, followed by fridge, freezer, and EWH*):
Apply GA optimizer with defined problem structure
Store optimized ON/OFF profile and resulting temperature dynamics
// Note: AC optimization result provides indoor temperature used by subsequent TCL models
END
Calculate cumulative energy consumption and cost for optimized solution
Display results (*temperature profiles, ON/OFF sequences, cumulative cost/energy plots*)
END

5. Demand Response considerations

The TCL optimization system presented in this study is designed to ensure that any microgrid containing it remains consistently available to participation in demand response programs, including load shifting, peak shaving, and demand flexibility. This work introduces and distinguishes two novel terms regarding TCLs: the operating temperature hysteresis band and the comfort temperature hysteresis band. The operating temperature hysteresis band refers to the range within which optimization occurs, and TCLs operate under normal conditions. This band is contained within the comfort temperature hysteresis band, which represents the less restrictive range for TCLs. TCLs can only operate within this band if a command is issued by the system operator to participate in a demand response event upon receipt of a grid request. The comfort temperature hysteresis band is imposed by the TCL user, as exceeding these temperature limits would compromise user comfort.

Fig. 6 illustrates the temperature dynamics within a system governed by a TCL. Following a designated demand response period, initially marked as t_{DR_i} and t_{DR_F} indicating the commencement and conclusion of the demand response, respectively, the TCL reverts to its optimization schedule. The restoration of the optimization schedule after the demand response is ensured by the supervisor described in section 6. The time at which it reaches the pre-defined on/off sequence for optimization is termed as the optimization recovery time $t_{o.r.}$. Furthermore, each THB mentioned previously is delineated by dashed lines in different colours.

To accurately anticipate the available resources for engaging in a demand response (DR) event upon receiving a grid request, and to ensure the consistent delivery of the committed load reduction or load increase services during the DR periods, several indices have been previously established in the literature [52 53]. These indices take into account factors such as the operating temperature of the system, which varies across the different TCLs, as well as the availability of energy resources (power and duration over time). This available energy is shaded in green in Fig. 6.

6. Mismatches in the real-time operation: TCĹs supervisor

In real-time operation, mismatches between predicted and actual energy consumption of TCLs can arise due to various factors, such as uncertainties in environmental conditions and deviations from anticipated user behaviour, as well as DR periods described in the previous section. These discrepancies pose significant challenges to the effective management of TCLs' ON/OFF sequences, as they can result in suboptimal performance and uncontrolled and unoptimized ON/OFF sequences. The supervisor, equipped with real-time monitoring capabilities and advanced control algorithms, acts as a decision-making entity responsible for adjusting TCL operation in response to those dynamic changes.

To address mismatches in real-time operation, the TCL supervisor employs an adaptive strategy that dynamically adjusts TCL operation to align with the established ON/OFF sequence. Specifically, when deviations occur due to human behaviour or environmental factors such as changes in irradiance, resulting in temperatures not accounted for in the predetermined sequence, the supervisory layer would intervene in real-time. Its role would be to ensure that the TCL's temperature adapts to the target set by the preceding optimization sequence. Once the desired temperature is reached, the TCL can resume following the established ON/OFF sequence. This control strategy effectively ensures that the TCL operates optimally according to the predetermined sequence, even in the face of unforeseen deviations.

In Fig. 7, the graphical representation illustrates the dynamics described earlier. Once a disturbance occurs, causing the system to deviate from the proposed optimal dynamics, indicated as t_{P_i}, the supervisor initiates operation. This disturbance persists for a duration during which the supervisor may not be able to maintain full control over the TCL. Upon the conclusion of the disturbance at t_{P_F}, the system responds effectively to the supervisor's control, swiftly guiding the system back to the optimal temperature to resume following the optimal sequence obtained from the problem. The time taken by the system to recover and adhere to the proposed temperature is termed as the optimization recovery time, denoted as $t_{o.r.}$.

Fig. 12. Scenario: TCL + RES. Temperature dynamics and it corresponds ON/OFF sequence of a) AC b) Fridge c) Freezer d) EWH.

After analysing Fig. 7 and its accompanying explanation, it becomes evident that the optimization approach proposed in this work can facilitate the task of a supervisor, by providing a clear optimal ON/OFF sequence with the associated temperature profile. This optimized sequence allows for a swift response to disturbances, ensuring efficient control over the system dynamics. In contrast, if the optimization were based on setting a setpoint temperature, the system's response to mismatches would be significantly more complex and challenging to manage.

7. Use case

This section presents the application of the proposed optimization strategy to a representative residential microgrid, composed of the four TCL described previously: an AC with a nominal power of 2,000 W, a refrigerator consuming 50 W, a freezer with a rated input of 60 W, and an EWH of 500 W. The microgrid is conceptually located in Huelva, Spain (latitude 37°N), a region with a Mediterranean climate, characterized by mild winters and high solar potential.

The simulation covers a full 24-hour period corresponding to December 15, 2023 (day 338 of the year). The optimization is performed on the previous day, using forecasts available on December 14 to

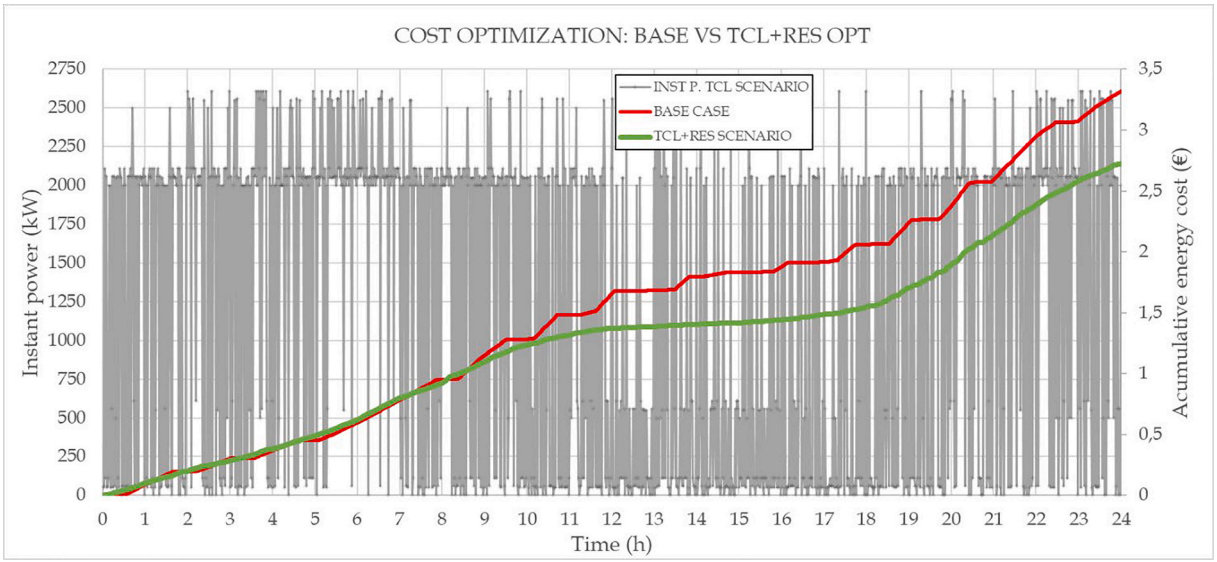

Fig. 13. Cumulative cost comparative between cases base (red) and the objective TCL + RES (green). (For interpretation of the references to colour in this figure legend, the reader is referred to the web version of this article.)

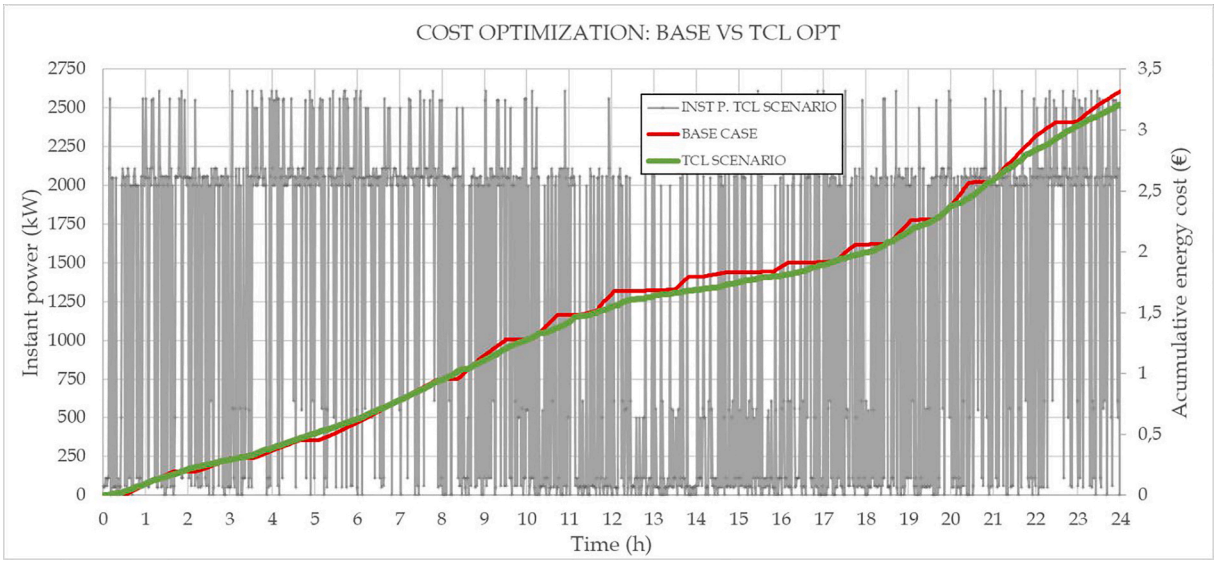

Fig. 14. Cumulative cost comparative between cases base (red) and the objective TCL (green). (For interpretation of the references to colour in this figure legend, the reader is referred to the web version of this article.)

determine the optimal ON/OFF switching sequence for the TCLs to be applied throughout December 15. All external inputs—ambient temperature, solar irradiance, and electricity prices—are based on day-ahead forecasts, in line with real-world scenarios where this information is published the day before operation. Weather data are sourced from the Spanish State Meteorological Agency (AEMET) [54], while the electricity price profile follows the official time-of-use (ToU) tariffs offered to residential consumers by Spanish utility providers [55]. The cold-water inlet temperature is dynamically estimated from the ambient temperature, ensuring consistency with the thermal behaviour of domestic appliances.

The optimization is applied to the microgrid composed of the four TCLs, considering the different configurations outlined in Table 6, which reflect varying levels of flexibility and resource integration. The remainder of this section is structured as follows: Section 7.1 introduces the external datasets used as inputs to the optimization; Section 7.2 presents the baseline scenario in which TCLs operate under fixed hysteresis control; and Section 7.3 compares this baseline with the optimized dispatch results across different microgrid configurations.

7.1. External Dataset Overview

The external inputs driving the optimization include irradiance (Is), ambient temperature (Tamb), and water temperature (Tw), all based on forecast data for the selected simulation day. These parameters are interpolated to a one-minute resolution to match the time discretization of the optimization algorithm and to capture the short-term dynamics of TCL operation with higher fidelity. The three environmental variables are shown in Fig. 8:

In addition to the weather-related inputs, electricity prices are incorporated as a key economic driver of the optimization. It is important to distinguish between the standard price signal, which reflects the utility's published ToU tariff, and the adjusted price, used in scenarios that account for renewable energy (RES) self-generation within the

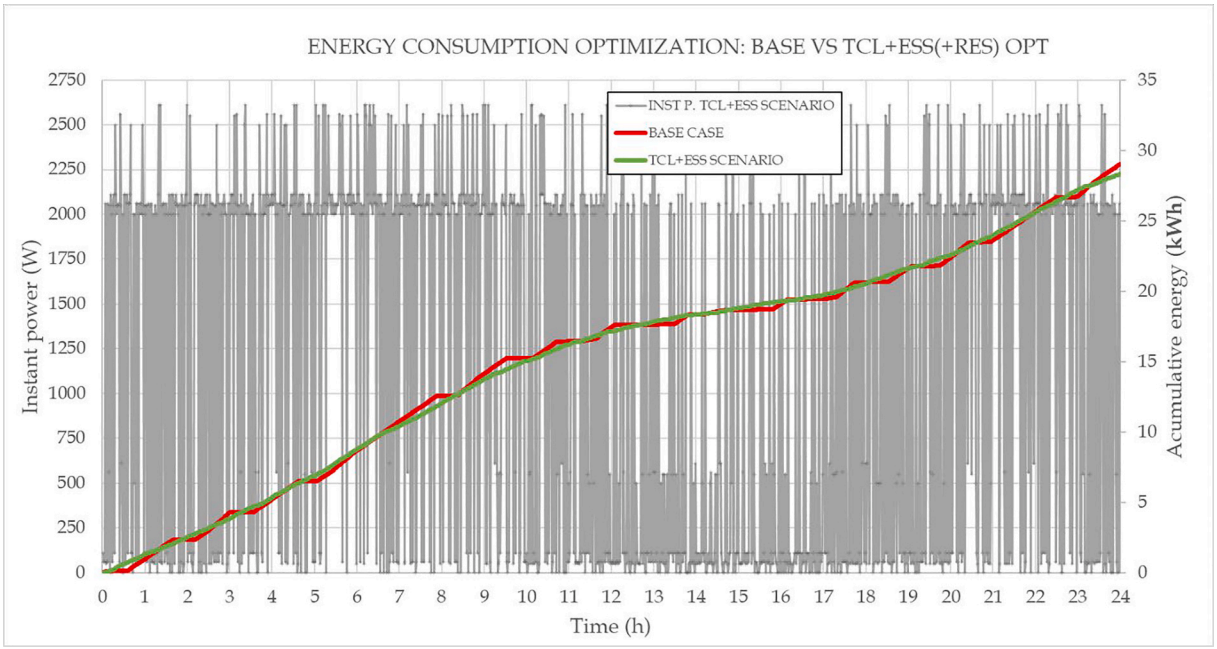

Fig. 15. Cumulative energy consumption comparative between cases base (red) and the objective TCL + ESS(+RES) (green). (For interpretation of the references to colour in this figure legend, the reader is referred to the web version of this article.)

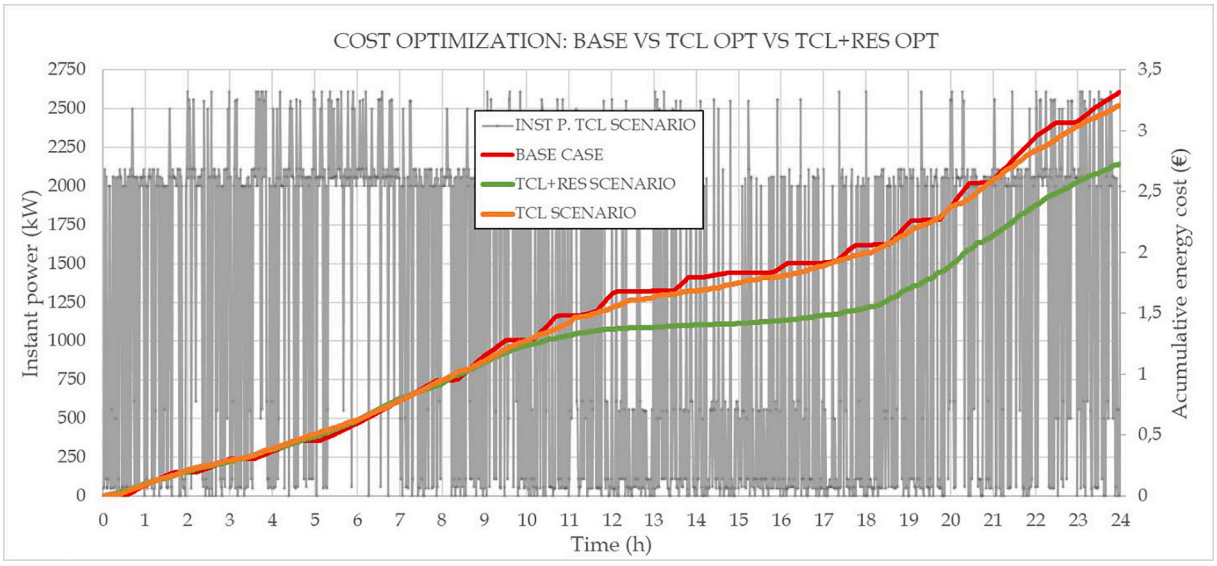

Fig. 16. Cumulative cost comparative between cases base (red), the objective TCL (orange) and the objective TCL + RES (green). (For interpretation of the references to colour in this figure legend, the reader is referred to the web version of this article.)

Table 7
Summary of optimization results for the use case under different microgrid scenarios.

Scenario	Objective	Improvement Achieved
TCL only	Energy cost minimization	3.3 % reduction in daily energy cost
TCL + RES	Energy cost minimization considering RES	18 % reduction in daily energy cost
TCL + ESS (and/ or RES)	Power consumption minimization	2.4 % reduction in daily energy consumption

microgrid. The adjusted price, illustrated in Fig. 9b, results from the equivalence defined in Equation (7) (Section 4.2, Objective 3), which reflects the economic value of self-consumed photovoltaic energy. In this context, a rooftop PV system is assumed to be available with an area of 24.2 m2 and an efficiency of 20 %, in line with typical residential installations.

The colour scale of the bars in Fig. 9 is computed automatically based on the range of electricity prices. Notably, even bars unaffected by RES production may exhibit colour variation between Fig. 9a and b due to dynamic rescaling.

7.2. *Baseline case: Fixed thermostatically load*

The TCLs operate within a base case scenario where the control

consists of maintaining the temperature objective into a band around the set point established by the user in each time. The band represents the comfort temperature range. This base case serves as a fundamental reference point for comparing against optimization scenarios because it reflects the standard operational protocols inherent in these appliances today.

7.3. Optimization cases

The optimization strategy flowchart used to optimize the ON/OFF sequence profile of the TCLs within the microgrid is depicted in Fig. 11. The evaluation primarily focuses on assessing the TCL's performance in terms of power consumption and energy costs. These two metrics represent key areas for potential microgrid enhancement, and the variables directly involved in the different objectives designed in section 3 and also exert a direct influence on the overall microgrid performance and efficiency.

7.3.1. Scenario: TCL + RES

The chosen scenario for in-depth study is the most complete, as previous scenarios only required specifying the microgrid's composition to the optimizer. In this case, it is necessary to specify the square meters of photovoltaic panel surface area and their efficiency. Additionally, the introduced prices are adjusted prices based on RES production, as illustrated in Fig. 9 b). The results obtained applying this objective are presented in Fig. 12 where can be seen temperature profiles very different from those corresponding to the base case shown in Fig. 10.

The graphs shown in Fig. 12 showcase the temperature profiles and ON/OFF sequences of each TCL, providing insights into their operational patterns and energy consumption behaviour. Fig. 13 illustrates a comparison between the cumulative energy costs in the base case and the TCL + RES optimization scenario.

This comparative graph highlights the significant reduction in energy costs achieved through optimization. As illustrated, by the end of the day, the optimized scenario marked in colour green, exhibits a 18 % decrease in costs compared to the base case.

7.3.2. All other scenarios

Only two other scenarios are considered for the other 3 cases of microgrid composition, as explained in section 3: the cost optimization in the case of a microgrid only composed of TCL and the energy consumption optimization in the cases in which the microgrid contains ESS. The results corresponding to the cost optimization in the cases of a microgrid only composed of TCLs is presented in Fig. 14. As can be seen, a perceptible decrease of the daily cost is obtained, which represents in the assess day a 3,3 %.

The results corresponding to the energy consumption optimization are presented in Fig. 15, where a decrease of 2,4 % in the daily energy consumption is obtained.

Finally, Fig. 16 presents the comparison between the two cost optimization algorithms presented, one of them without considering the RES production and the other promoting the consume during the hours in which the RES are generating energy. As can be seen the second optimization objective obtain much better results.

To better illustrate the improvements achieved for the use case through the proposed optimization strategy across the different microgrid compositions, Table 7 summarizes the key results. The reductions in both energy costs and consumption demonstrate the effectiveness and adaptability of the approach for various scenarios.

8. Conclusions

In this study, the optimization of microgrids has been explored, with particular emphasis on the dispatch of thermostatically controllable loads (TCLs) commonly found in residential settings. The optimization objectives have been carefully crafted to accommodate the diverse compositions of microgrids, whether they include renewable energy systems (RES), energy storage systems (ESS), or consist solely of loads. Notably, the approach considers the TCLs' potential contribution to demand response programs within the broader power system context, while also addressing the challenges stemming from discrepancies between day-ahead dispatch instructions and real-time operational conditions.

A key element of this optimization process lies in the utilization of a genetic algorithm (GA) to determine optimal on/off sequences and corresponding temperature profiles for each TCL. Unlike traditional approaches based on variable temperature setpoints, this method prioritizes the optimization of energy consumption or energy costs, enabling TCLs to seamlessly participate in demand response activities and adapt to unforeseen events while maintaining optimized performance profiles.

Future research endeavours will focus on enhancing the optimization framework to incorporate representations of human behaviour within smart-home settings. A key objective will be to transition from simulation optimization to practical implementation by integrating a real-time supervisor control system, deploying, and testing the proposed optimization algorithm directly within laboratory-scale microgrid networks.

CRediT authorship contribution statement

Jesus Clavijo-Camacho: Writing – original draft, Software, Methodology, Investigation, Conceptualization. **Gabriel Gomez-Ruiz:** Writing – review & editing, Software, Investigation, Data curation. **J.A. Hernández Torres:** Writing – review & editing, Validation, Investigation. **Reyes Sanchez-Herrera:** Writing – review & editing, Supervision, Project administration, Investigation.

Declaration of competing interest

The authors declare that they have no known competing financial interests or personal relationships that could have appeared to influence the work reported in this paper.

Acknowledgements

This research was supported by the grant PID2020-117828RB-I00 funded by MICIU/AEI/10.13039/501100011033 and, by the Spanish Ministry of Science, Innovation and Universities. The author Jesus Clavijo-Camacho is enjoying a "INVESTIGO" research fellowship funded by the European Commission - NextGenerationEU. In addition, the author Gabriel Gómez-Ruiz is enjoying an FPU grant, number FPU21/00468, funded by the Spanish Ministry of Science, Innovation and Universities for the training of university teaching staff during his PhD period. Funding for open access charge: Universidad de Huelva / CBUA.

Data availability

Data will be made available on request.

References

[1] A. Sinha, M. Shahbaz, T. Sengupta, Renewable energy policies and contradictions in causality: a case of next 11 countries, J. Clean. Prod. 197 (Oct. 2018) 73–84, https://doi.org/10.1016/j.jclepro.2018.06.219.

[2] 'Electricity from renewable sources up to 41% in, Eurostat' https://ec.europa.eu/eurostat/web/products-eurostat-news/w/ddn-20240221-1 2022 Accessed: May 03, 2024. [Online]. Available:.

[3] 'Solar PV and wind supply about 40% of building electricity use by 2030 – Analysis', IEA. Accessed: May 03, 2024. [Online]. Available: https://www.iea.org/reports/solar-pv-and-wind-supply-about-40-of-building-electricity-use-by-2030.

[4] P. Neetzow, The effects of power system flexibility on the efficient transition to renewable generation, Appl. Energy 283 (Feb. 2021) 116278, https://doi.org/10.1016/j.apenergy.2020.116278.

[5] M. Seatle, M. Mcpherson, Residential demand response program modelling to compliment grid composition and changes in energy efficiency, Energy 290 (Mar. 2024) 130173, https://doi.org/10.1016/j.energy.2023.130173.

[6] T.N. Duy, M. Negnevitsky, M. de Groot, Pool-based demand Response Exchange-Concept and Modeling, IEEE Trans. Power Syst. 26 (3) (Aug. 2011) 1677–1685, https://doi.org/10.1109/TPWRS.2010.2095890.

[7] J. Wang, Y. Shi, Y. Zhou, Intelligent demand Response for Industrial Energy Management considering Thermostatically Controlled Loads and EVs, IEEE Trans. Ind. Inform. 15 (6) (Jun. 2019) 3432–3442, https://doi.org/10.1109/TII.2018.2875866.

[8] S. A. B. dos Santos, J. M. Soares, G. C. Barroso, and B. de A. Prata, 'Demand response application in industrial scenarios: A systematic mapping of practical implementation', *Expert Syst. Appl.*, vol. 215, p. 119393, Apr. 2023, doi: 10.1016/j.eswa.2022.119393.

[9] B. Mohandes, S. Acharya, M.S. El Moursi, A.S. Al-Sumaiti, H. Doukas, S. Sgouridis, Optimal Design of an Islanded Microgrid with Load Shifting Mechanism between Electrical and Thermal Energy Storage Systems, IEEE Trans. Power Syst. 35 (4) (Jul. 2020) 2642–2657, https://doi.org/10.1109/TPWRS.2020.2969575.

[10] X. Zhu, P. Wang, N. Li, W. Yan, Multi-period optimal scheduling of building loads based on accurate virtual battery model, Energy and Buildings 327 (Jan. 2025) 115046, https://doi.org/10.1016/j.enbuild.2024.115046.

[11] D.P. Chassin, J. Stoustrup, P. Agathoklis, N. Djilali, A new thermostat for real-time price demand response: cost, comfort and energy impacts of discrete-time control without deadband, Applied Energy 155 (Oct. 2015) 816–825, https://doi.org/10.1016/j.apenergy.2015.06.048.

[12] B. Aluisio, M. Dicorato, G. Forte, G. Litrico, M. Trovato, Integration of heat production and thermal comfort models in microgrid operation planning, Sustain. Energy Grids Netw. 16 (Dec. 2018) 37–54, https://doi.org/10.1016/j.segan.2018.05.004.

[13] R. Morsali, G.S. Thirunavukkarasu, M. Seyedmahmoudian, A. Stojcevski, R. Kowalczyk, A relaxed constrained decentralised demand side management system of a community-based residential microgrid with realistic appliance models, Appl. Energy 277 (Nov. 2020) 115626, https://doi.org/10.1016/j.apenergy.2020.115626.

[14] A. Kumar, A.R. Singh, R.S. Kumar, Y. Deng, X. He, R.C. Bansal, P. Kumar, R. M. Naidoo, An effective energy management system for intensified grid-connected microgrids, Energy Strateg. Rev. 50 (Nov. 2023) 101222, https://doi.org/10.1016/j.esr.2023.101222.

[15] H. Shuai, J. Fang, X. Ai, Y. Tang, J. Wen, H. He, Stochastic Optimization of Economic Dispatch for Microgrid based on Approximate Dynamic programming, IEEE Trans. Smart Grid 10 (3) (May 2019) 2440–2452, https://doi.org/10.1109/TSG.2018.2798039.

[16] X. Xue, J. Fang, X. Ai, S. Cui, Y. Jiang, W. Yao, J. Wen, A fully distributed ADP Algorithm for Real-Time Economic Dispatch of Microgrid, IEEE Trans. Smart Grid 15 (1) (Jan. 2024) 513–528, https://doi.org/10.1109/TSG.2023.3273418.

[17] T.H.B. Huy, H.T. Dinh, D.N. Vo, D. Kim, Real-time energy scheduling for home energy management systems with an energy storage system and electric vehicle based on a supervised-learning-based strategy, Energy Conv. Manag. 292 (Sep. 2023) 117340, https://doi.org/10.1016/j.enconman.2023.117340.

[18] Z. Luo, J. Peng, R. Yin, Many-objective day-ahead optimal scheduling of residential flexible loads integrated with stochastic occupant behavior models, Applied Energy 347 (Oct. 2023) 121348, https://doi.org/10.1016/j.apenergy.2023.121348.

[19] D.G. Rosero, N.L. Diaz, C.L. Trujillo, Cloud and machine learning experiments applied to the energy management in a microgrid cluster, Appl. Energy 304 (Dec. 2021) 117770, https://doi.org/10.1016/j.apenergy.2021.117770.

[20] Z. A. Obaid, L. Cipcigan, and M. T. Muhssin, 'Design of a hybrid fuzzy/Markov chain-based hierarchal demand-side frequency control', in *2017 IEEE Power & Energy Society General Meeting*, Jul. 2017, pp. 1–5. doi: 10.1109/PESGM.2017.8273821.

[21] Y. Ji, J. Wang, J. Xu, D. Li, Data-Driven Online Energy Scheduling of a Microgrid based on Deep Reinforcement Learning, Energies 14 (8) (Apr. 2021) 2120, https://doi.org/10.3390/en14082120.

[22] H. Zhang, S. Seal, D. Wu, F. Bouffard, B. Boulet, Building Energy Management with Reinforcement Learning and Model Predictive Control: a Survey, IEEE Access 10 (2022) 27853–27862, https://doi.org/10.1109/ACCESS.2022.3156581.

[23] J. Zhang, D. Qin, Y. Ye, Y. He, X. Fu, J. Yang, G. Shi, H. Zhang, Multi-Time Scale Economic Scheduling Method based on Day-Ahead Robust Optimization and Intraday MPC Rolling Optimization for Microgrid, IEEE Access 9 (2021) 140315–140324, https://doi.org/10.1109/ACCESS.2021.3118716.

[24] Y. Zhang, F. Meng, R. Wang, B. Kazemtabrizi, J. Shi, Uncertainty-resistant stochastic MPC approach for optimal operation of CHP microgrid, Energy 179 (Jul. 2019) 1265–1278, https://doi.org/10.1016/j.energy.2019.04.151.

[25] J. Yang, Z. Li, K. Ma, H. Li, Z. Jiao, Encouraging thermostatically controlled loads to provide frequency regulation for smart grid: a comfort-level trading mechanism, Expert Systems with Applications 249 (Sep. 2024) 123618, https://doi.org/10.1016/j.eswa.2024.123618.

[26] Z. Ullah, K. Ullah, G. Gruosso, Using Controlled Thermostatic Loads in buildings as Auxiliary Services to the Power Grid: an Investigation with Thoroughly simulated Case Study, International Journal of Energy Research 2024 (1) (2024) 5581128, https://doi.org/10.1155/er/5581128.

[27] S. Pang, Z. Zheng, X. Xiao, C. Huang, S. Zhang, J. Li, Y. Zong, S. You, Collaborative power tracking method of diversified thermal loads for optimal demand response: a MILP-Based decomposition algorithm, Applied Energy 327 (Dec. 2022) 120006, https://doi.org/10.1016/j.apenergy.2022.120006.

[28] H. Xiao, M. Zhang, L. Zeng, G. Wu, C. Wu, C. Wu, Hierarchical control strategy of thermostatically controlled load considering multiple factors, Energy and Buildings 291 (Jul. 2023) 113148, https://doi.org/10.1016/j.enbuild.2023.113148.

[29] X. Mao, M. Xue, T. Zhang, W. Tan, Z. Zhang, Y. Pan, H. Wu, Z. Lin, Centralized bidding mechanism of demand response based on blockchain, Energy Rep. 8 (Aug. 2022) 111–117, https://doi.org/10.1016/j.egyr.2022.02.145.

[30] K. Sakurama, M. Miura, Communication-based Decentralized demand Response for Smart Microgrids, IEEE Trans. Ind. Electron. 64 (6) (Jun. 2017) 5192–5202, https://doi.org/10.1109/TIE.2016.2631133.

[31] Z. Meng, T. Pan, W. Zhou, X. Jin, J. Hou, W. Cao, K. Li, Decentralized control strategy of thermostatically controlled loads considering the energy efficiency ratio and measurement error correction, Front. Energy Res. 12 (May 2024), https://doi.org/10.3389/fenrg.2024.1375715.

[32] L. Massidda, M. Marrocu, Hybrid forecasting of demand flexibility: a top-down approach for thermostatically controlled loads, Energy and AI 20 (May 2025) 100487, https://doi.org/10.1016/j.egyai.2025.100487.

[33] A. Elkasrawy, B. Venkatesh, Positive demand response and multi-hour net benefit test, Electr. Power Syst. Res. 183 (Jun. 2020) 106275, https://doi.org/10.1016/j.epsr.2020.106275.

[34] A. Zakariazadeh, O. Homaee, S. Jadid, P. Siano, A new approach for real time voltage control using demand response in an automated distribution system, Appl. Energy 117 (Mar. 2014) 157–166, https://doi.org/10.1016/j.apenergy.2013.12.004.

[35] S.M. Ghorashi, M. Rastegar, S. Senemmar, A.R. Seifi, Optimal design of reward-penalty demand response programs in smart power grids, Sust. Cities Soc. 60 (Sep. 2020) 102150, https://doi.org/10.1016/j.scs.2020.102150.

[36] D. Xu, F. Zhong, Z. Bai, Z. Wu, X. Yang, M. Gao, Real-time multi-energy demand response for high-renewable buildings, Energy and Buildings 281 (Feb. 2023) 112764, https://doi.org/10.1016/j.enbuild.2022.112764.

[37] K. Xie, H. Hui, Y. Ding, Review of modeling and control strategy of thermostatically controlled loads for virtual energy storage system, Protection and Control of Modern Power Systems 4 (1) (Dec. 2019) 23, https://doi.org/10.1186/s41601-019-0135-3.

[38] G. Fambri, P. Marocco, M. Badami, D. Tsagkrasoulis, The flexibility of virtual energy storage based on the thermal inertia of buildings in renewable energy communities: a techno-economic analysis and comparison with the electric battery solution, J. Energy Storage 73 (Dec. 2023) 109083, https://doi.org/10.1016/j.est.2023.109083.

[39] X. Kong, B. Sun, J. Zhang, S. Li, Q. Yang, Power retailer Air-Conditioning load Aggregation operation Control Method and demand Response, IEEE Access 8 (2020) 112041–112056, https://doi.org/10.1109/ACCESS.2020.3003278.

[40] Z. Yin, Y. Che, D. Li, H. Liu, D. Yu, Optimal Scheduling Strategy for Domestic Electric Water Heaters based on the Temperature State Priority list, Energies 10 (9) (Sep. 2017) 1425, https://doi.org/10.3390/en10091425.

[41] M. Song, C. Gao, M. Shahidehpour, Z. Li, J. Yang, H. Yan, State Space Modeling and Control of Aggregated TCLs for Regulation Services in Power Grids, IEEE Trans. Smart Grid 10 (4) (Jul. 2019) 4095–4106, https://doi.org/10.1109/TSG.2018.2849321.

[42] A. Mirakhorli, B. Dong, Occupancy behavior based model predictive control for building indoor climate—A critical review, Energy and Buildings 129 (Oct. 2016) 499–513, https://doi.org/10.1016/j.enbuild.2016.07.036.

[43] Z. Xu, R. Diao, S. Lu, J. Lian, Y. Zhang, Modeling of Electric Water Heaters for demand Response: a Baseline PDE Model, IEEE Transactions on Smart Grid 5 (5) (Sep. 2014) 2203–2210, https://doi.org/10.1109/TSG.2014.2317149.

[44] C.J.L. Hermes, C. Melo, F.T. Knabben, J.M. Gonçalves, Prediction of the energy consumption of household refrigerators and freezers via steady-state simulation, Applied Energy 86 (7) (Jul. 2009) 1311–1319, https://doi.org/10.1016/j.apenergy.2008.10.008.

[45] M. Luo, K. Jiang, J. Wang, W. Feng, L. Ma, X. Shi, X. Zhou, Data-driven thermal preference prediction model with embodied air-conditioning sensors and historical usage behaviors, Building and Environment 220 (Jul. 2022) 109269, https://doi.org/10.1016/j.buildenv.2022.109269.

[46] B. Lin, S. Li, and Y. Xiao, 'Optimal and Learning-Based Demand Response Mechanism for Electric Water Heater System', *Energies*, vol. 10, no. 11, Art. no. 11, Nov. 2017, doi: 10.3390/en10111722.

[47] G. T. Costanzo, F. Sossan, M. Marinelli, P. Bacher, and H. Madsen, 'Grey-box modeling for system identification of household refrigerators: A step toward smart appliances', in *2013 4th International Youth Conference on Energy (IYCE)*, Jun. 2013, pp. 1–5. doi: 10.1109/IYCE.2013.6604197.

[48] F. Sossan, V. Lakshmanan, G.T. Costanzo, M. Marinelli, P.J. Douglass, H. Bindner, Grey-box modelling of a household refrigeration unit using time series data in application to demand side management, Sustainable Energy, Grids and Networks 5 (Mar. 2016) 1–12, https://doi.org/10.1016/j.segan.2015.10.003.

[49] G. Gomez-Ruiz, R. Sanchez-Herrera, J. M. Andujar, and J. L. Rubio Sanchez, 'Simulation-Based Education Tool for Understanding Thermostatically Controlled Loads', *Sustainability*, vol. 16, no. 3, Art. no. 3, Jan. 2024, doi: 10.3390/su16030999.

[50] P. Du, N. Lu, Appliance Commitment for Household load Scheduling, IEEE Transactions on Smart Grid 2 (2) (Jun. 2011) 411–419, https://doi.org/10.1109/TSG.2011.2140344.

[51] C.D. Korkas, M. Terzopoulos, C. Tsaknakis, E.B. Kosmatopoulos, Nearly optimal demand side management for energy, thermal, EV and storage loads: an Approximate Dynamic programming approach for smarter buildings, Energy and Buildings 255 (Jan. 2022) 111676, https://doi.org/10.1016/j.enbuild.2021.111676.

[52] X. Jin, K. Baker, D. Christensen, S. Isley, Foresee: a user-centric home energy management system for energy efficiency and demand response, Applied Energy 205 (Nov. 2017) 1583–1595, https://doi.org/10.1016/j.apenergy.2017.08.166.

[53] J. Wang, Y. Jiang, C.Y. Tang, L. Song, Analysis of predicted mean vote-based model predictive control for residential HVAC systems, Build. Environ. 229 (Feb. 2023) 109952, https://doi.org/10.1016/j.buildenv.2022.109952.

[54] A. E. de Meteorología, 'Agencia Estatal de Meteorología - AEMET. Gobierno de España'. Accessed: Mar. 26, 2025. [Online]. Available: https://www.aemet.es/es/portada.

[55] 'PVPC | ESIOS electricidad · datos · transparencia'. Accessed: Mar. 26, 2025. [Online]. Available: https://www.esios.ree.es/es/pvpc.